International Journal of Signal Processing, Image Processing and Pattern Recognition
Vol. 7, No. 6 (2014), pp. 51-64
http://dx.doi.org/10.14257/ijsip.2014.7.6.05

Fractional Differentiation-based Image Feature Extraction

Xiangwei Xu[1,*], Fang Dai[1], Jianmin Long[2] and Wenyan Guo[1]

[1] *School of Science, Xi'an University of Technology, Xi'an 710054, China*
[2] *Department of Engineering Mechanics, SVL, Xi'an Jiaotong University, Xi'an 710049, China*
xuxwei69@163.com, daifang@xaut.edu.cn

Abstract

Two novel methods for image feature extraction based on fractional differentiation are presented in this paper. The first method is the feature extraction of fusing multi-direction CRONE operators. In this method, the fractional differential CRONE mask is generalized to eight directions at first for extracting image features; then the extracted features are tested by the statistic method and fused by the gradient ratio, so that the outlines of the objects in the image are obtained. In order to extract the detail feature information in the image effectively, the second method, the 'S+Z' extraction combined with the space-filling curves, is presented. By introducing the space-filling curves, the 'S' curve and the 'Z' curve, and making full use of the neighborhood information of image pixels, the detailed features of the objects in the image are obtained. The experiment results show that our methods can obtain satisfactory image features.

Keywords: *feature extraction; fractional differentiation; multi-direction extraction; space-filling curve*

1. Introduction

As an important branch of mathematical analysis, fractional differentiation was presented almost at the same time with integral order differentiation, and can date back to at the correspondence between L'Hôpital and Leibniz three hundred years ago. Since then, fractional differentiation has been studied by many researchers from different views, and the most widely used definitions are the Riemann-Liouville (R-L) fractional differentiation, the Grümwald-Letnikov (G-L) fractional differentiation and the Caputo fractional differentiation [1]. As the proposing of fractal theory by Mandelbrot in 1970s [2], fractional differentiation has been applied in many subjects, such as mechanics, chemistry, economics, etc., especially in control theory and robotics.

The researches on the amplitude-frequency characteristics of signals after the processing of fractional differentiation show that, when the value of fractional order n is small ($0<n<1$), fractional differentiation processing can greatly enhance the high frequency components, reinforce the medium frequency components and nonlinearly keep the low frequency components of signals [3], which indicates that fractional differentiation has a wide range of applications in the field of image processing [4, 5]. The pioneer work of the application of fractional differentiation in the field of image processing is done by Mathieu et al. who used the CRONE operator, a fractional differential operator designed by Oustaloup at the end of 20th

* Corresponding Author

ISSN: 2005-4254 IJSIP

century, to extract the image edges [6]. Up to now, though fractional differentiation has been used in the area of image segmentation [7, 8], image denoising [9, 10], image enhancement [11, 12], *etc.*, it is still in its infancy [13], and is seldom used in the field of image feature extraction.

In this paper, the horizontal mask of the CRONE operator is generalized to eight directions to extract image features; then the extracted features are tested by the statistic method to eliminate the ineffective features and fused by the gradient ratio to obtain feature results [14, 15]. This extraction method can extract the outlines of the objects in the image effectively, and has a good performance on the feature extraction of images like head portraits, traffic scenes, etc. On the other hand, for making full use of the neighborhood information of image pixels, the 'S' curve, a kind of space-filling curve in fractal geometry [16], is introduced. According to the 'S' curve, the coefficients of fractional differential CRONE mask is rearranged to construct a 3×3 mask for image feature extraction. To avoid of neglecting image features in the direction of 135 degrees when the mask constructed according to the 'S' curve is only used, the mask constructed according to the 'Z' curve, which is symmetrical to the 'S' curve, is used in combination to extract image features comprehensively. This 'S+Z' extraction method can extract the detail feature information of images effectively, and can be applied to texture feature extraction of images.

2. Multi-direction Feature Extraction based on CRONE Operator

2.1. CRONE Operator

For the application of fractional differentiation in the field of image processing, Mathieu et al. developed the CRONE operator as [6]

$$\underset{\leftrightarrow}{D}^{\alpha} = \frac{1}{h^{\alpha}} \sum_{k=0}^{\infty} (-1)^k \binom{\alpha}{k} (q^{-k} - q^{k}), \tag{1}$$

where the spatial operator $\underset{\leftrightarrow}{D}^{\alpha}$ represents the difference between the αth derivative for increasing x and the αth derivative for decreasing x of a transition $f(x)$, h is the step size, q is the shift operator defined as

$$qf(x) = f(x+h) \quad \text{or} \quad q^{-1} f(x) = f(x-h). \tag{2}$$

Using $\underset{\leftrightarrow}{D}^{\alpha}$ to a transition $f(x)$ and then we get

$$\underset{\leftrightarrow}{D}^{\alpha} f(x) = \frac{1}{h^{\alpha}} \sum_{k=0}^{\infty} a_k [f(x-kh) - f(x+kh)], \tag{3}$$

where

$$a_k = (-1)^k \binom{\alpha}{k} = (-1)^k \frac{\alpha(\alpha-1)\mathrm{L}\ (\alpha-k+1)}{k!}.$$

For a given α, a_k decreases to zero with the increasing of k; that is, the influence of a_k on $f(x-kh)$ and $f(x+kh)$ diminish with the increasing of k. So Eq. (3) can be approximated with finite terms and the CRONE formula is obtained as

$$\underset{\leftrightarrow}{D}^{\alpha} f(x) \approx \frac{1}{h^{\alpha}} \sum_{k=0}^{m} a_k [f(x-kh) - f(x+kh)]. \tag{4}$$

For the application of CRONE formula in image processing, the coefficients of Eq. (4) are arranged as the mask form, as shown in Fig. 1 (a). Setting h=1, the mask size then will be $2m$+1.

2.2. Multi-direction Feature Extraction

Generally, the CRONE mask is used to extract image features along the horizontal and vertical directions, and the extracted features are not satisfactory. Therefore, the CRONE mask is generalized to multi-directions to extract features. As the initial mask, the CRONE mask (Figure 1(a)) is rotated anticlockwise every $\pi/8$ and masks in eight directions are obtained, as shown in Figure 1(b).

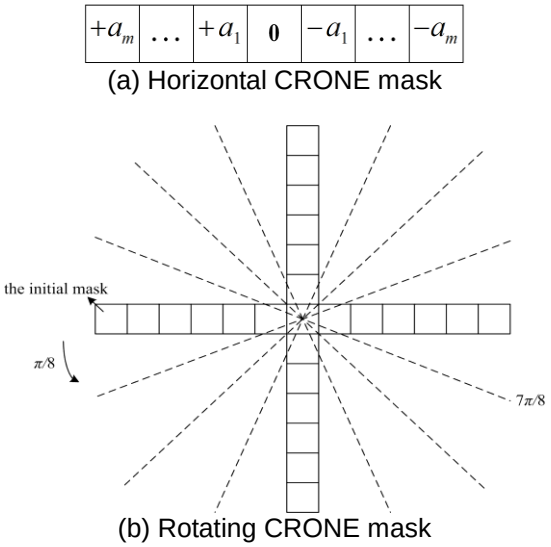

(a) Horizontal CRONE mask

(b) Rotating CRONE mask

Figure 1. CRONE Mask

The coefficients of the eight masks are labeled as $f_{k\pi/8}(n)$ (k=0,1, …,7), where n=1,…,2m+1 represents the location of the pixel inside each mask, and the corresponding gray values are denoted as c_n. The magnitude for each mask on the corresponding pixel can be obtained as

$$b_k = \sum_{n=1}^{2m+1} c_n f_{k\pi/8}(n). \tag{5}$$

It should be pointed out that, there may be no corresponding pixels in the image for the mask coefficients when features are extracted along the direction of $k\pi/8$ (k=1, 3, 5, 7). To solve this problem, we use the linear interpolation of the nearest two pixels to replace the corresponding pixel, as shown in Figure 2.

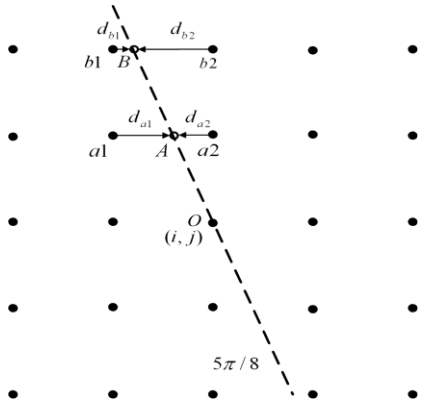

Figure 2. Interpolation on the Direction of $5\pi/8$

As can be seen in Figure 2, pixel $O(i, j)$ is the location of the mask centre, A and B are the pixels to be interpolated and the gray values of which can be interpolated as

$$p(A) = \frac{d_{a1}}{d_{a1} + d_{a2}} p(a1) + \frac{d_{a2}}{d_{a1} + d_{a2}} p(a2),$$

$$p(B) = \frac{d_{b1}}{d_{b1} + d_{b2}} p(b1) + \frac{d_{b2}}{d_{b1} + d_{b2}} p(b2), \quad (6)$$

where a_1 and a_2 are the nearest two pixels of pixel A, d_{a1} and d_{a2} are the distances between them and pixel A; b_1 and b_2 are the nearest two pixels of pixel B, d_{b1} and d_{b2} are the distances between them and pixel B, respectively.

Figures 3 (b) ~ (i) are the feature results of Figure 3 (a) extracted by the CRONE operator along eight directions, where m=2, α=0.55. It can be seen in Figures 3 (b) ~ (i) that there are some false or unimportant features in the eight feature results. Therefore, a criterion is needed to test the eight feature results and reject these false or unimportant features.

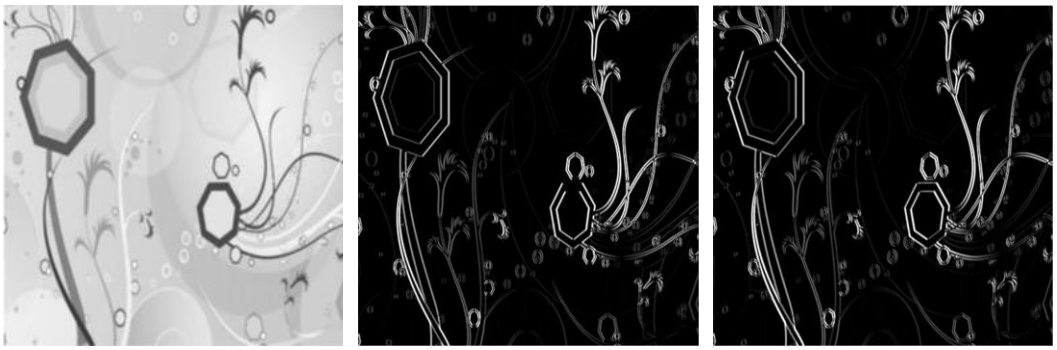

(a) Original image (b) The feature result of 0° (c) The feature result of $\pi/8$

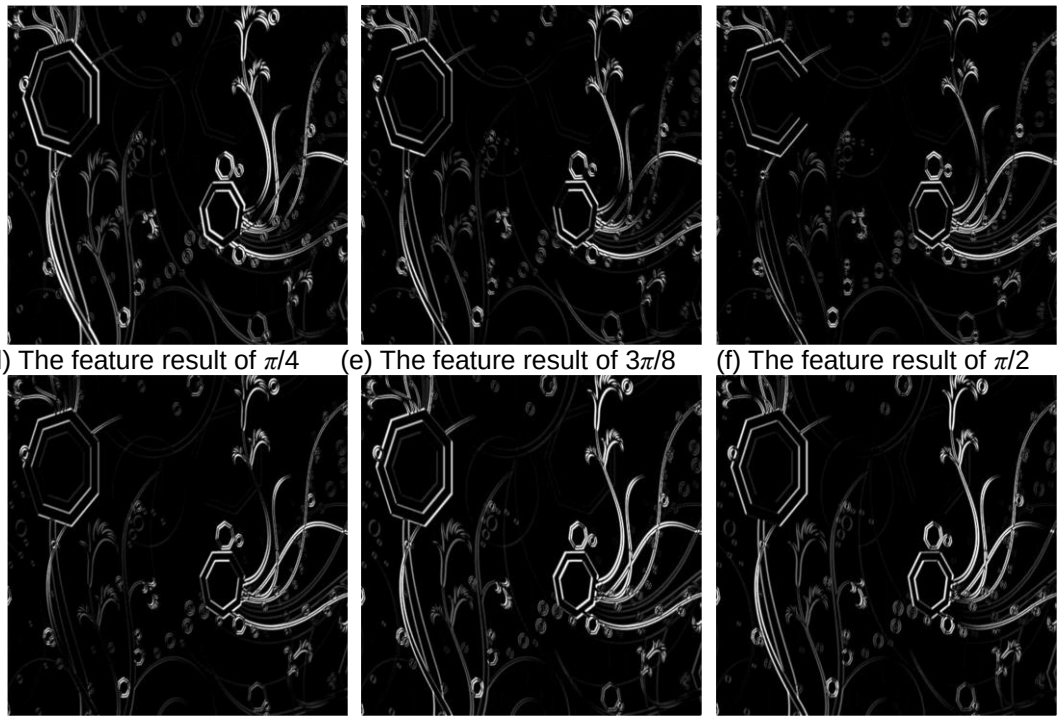

(d) The feature result of $\pi/4$ (e) The feature result of $3\pi/8$ (f) The feature result of $\pi/2$

(g) The feature result of $5\pi/8$ (h) The feature result of $3\pi/4$ (i) The feature result of $7\pi/8$

Figure 3. Feature Results of CRONE Extraction on Eight Directions

2.3. Feature Test

The features to be tested are assumed as a region with a length l and a width w and there are three hypotheses [14]:

H_1: feature region locates at the middle position of a homogeneous region,

H_2: feature region locates at the middle position of two homogeneous regions,

H_3: feature region locates at the middle position of three homogeneous regions,

as shown in Figure 4, where D_1^h is the image patch corresponding to the pixels of the homogeneous region, n_1^h is its number of pixels; D_2^{el} and D_2^{er} are the regions in the image corresponding to the pixels located to the left and right of the longest symmetry axis of the features to be tested, n_2^{el} and n_2^{er} are their number of pixels, respectively; D_3^s is the region in the image corresponding to the pixels of the features to be tested, D_3^{sl} and D_3^{sr} are the regions in the image corresponding to the pixels at the left and right of the features to be tested, n_3^s, n_3^{sl}, and n_3^{sr} are their number of pixels, respectively.

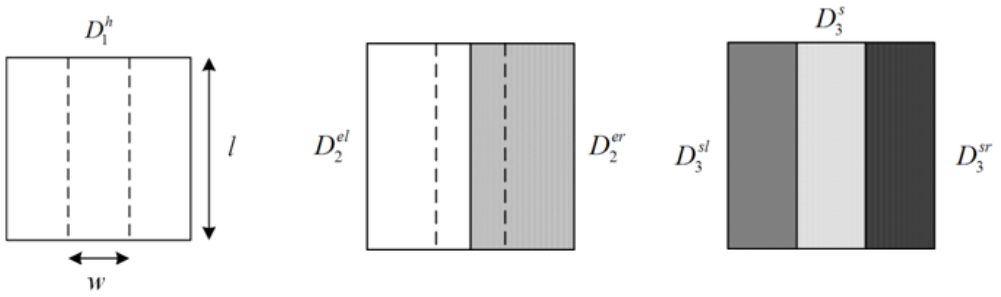

(a) H_1 (b) H_2 (c) H_3

Figure 4. Test Mask

By selecting the perpendicular direction of the extraction direction as the test direction and tracking the features along the test direction, the length and location of the feature region are determined. The log likelihood functions of the test hypotheses H_1, H_2 and H_3 can be written as [15]

$$\log L(H_1) = -\frac{n_1^h}{2} - n_1^h \log(\sigma_1^h \sqrt{2\pi}),$$

$$\log L(H_2) = -\frac{n_2^{er} + n_2^{el}}{2} - n_2^{er} \log(\sigma_2^{er} \sqrt{2\pi}) - n_2^{el} \log(\sigma_2^{el} \sqrt{2\pi}),$$

$$\log L(H_3) = -\frac{n_3^s + n_3^{sr} + n_3^{sl}}{2} - n_3^s \log(\sigma_3^s \sqrt{2\pi}) - n_3^{sr} \log(\sigma_3^{sr} \sqrt{2\pi}) - n_3^{sl} \log(\sigma_3^{sl} \sqrt{2\pi}),$$

(7)

where σ_1^h, σ_2^{el}, σ_2^{er}, σ_3^s, σ_3^{sl} and σ_3^{sr} are the parameter estimates of the standard deviations of the corresponding regions, respectively. Define the test statistics as

$$U(s) = \max\{\log L(H_3), \log L(H_2), \log L(H_1)\}. \quad (8)$$

If $U(s)=\log L(H_1)$, then the features to be tested are considered as false or unimportant features and should be rejected.

Figures 5 (a) ~ (h) are the testing results of the eight feature results in Figure 3. It can be seen in Figure 5 that the features on the main directions are detected.

(a) The testing result of $\pi/2$ (b) The testing result of $5\pi/8$ (c) The testing result of $3\pi/4$

(d) The testing result of $7\pi/8$ (e) The testing result of 0° (f) The testing result of $\pi/8$

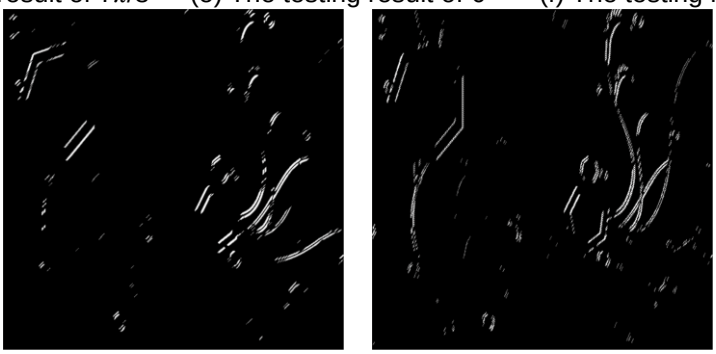

(g) The testing result of $\pi/4$ (h) The testing result of $3\pi/8$

Figure 5. Testing Results of the Eight Feature Results in Figure 3

2.4. Feature Fusion

How to fuse the eight feature results after being tested? The simplest fusion method is based on the 'OR' criterion, but has a shortcoming of fusing all features without choice. To avoid this shortcoming, the fusion method based on the distribution of gradient ratio is employed to fuse the eight feature results after being tested. The gradients g_k on the eight directions of $k\pi/8$ (k=0, 1, 2, …, 7) of the original image can be calculated by

$$g_k = C * A, \tag{9}$$

where A=[-1, 0, 1] is the gradient mask, C is the vector consisted of three gray values of the corresponding pixel.

Then the final feature result I is obtained by fusing features in the eight feature results after being tested

$$I = \sum_{k=0}^{7} r_k \cdot Ib_k, \tag{10}$$

where

$$r_k = \frac{g_k}{\sum_{k=0}^{7} g_k}, \tag{11}$$

are the gradient ratios, Ib_k are the test results of b_k in section 2.2. Figure 6 is the fusion result of Figures 5 (a) ~ (h), and the outlines of the objects in the image can be seen clearly.

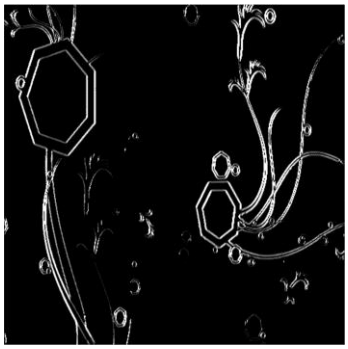

Figure 6. The Fusion Result of Figures 5 (a) ~ (h)

The above mentioned extraction method is now employed to extract features of the traffic scene, as shown in Figure 7 (a). Figure 7 (b) is the feature extraction result.

(a)Original image

(b) The feature extraction result

Figure 7. The Extraction Result of the Traffic Scene

It can be seen in Figure 7 (b) that the major features of the scene such as vehicle, road marking, etc., are extracted, but the detail features such as the bus number are obscure. The main reason for this shortcoming is that the above method breaks the continuity of the neighborhood information of image pixels in the process of feature extraction, and thus weakens the ability to extract the detail features of the image. In order to overcome this disadvantage, the 'S+Z' extraction method is presented with a full use of the neighborhood information of image pixels.

3. CRONE Operator based 'S+Z' Extraction Method

3.1. 'S' Curve based New Mask

A curve covering all points in a plane no-repeatedly is known as the space-filling curve in the fractal geometry, which is self-similar and can convert 2D plane and 1D curve into each other. The 'S' curve, as shown in Figure 8, is the basic part of the classic Peano space-filling curve [16] and can pass all points in a plane continuously and no-repeatedly.

The 3×3 mask is usually used for image feature extraction for two reasons. One is the center point in a mask of this size can be determined as the point to be extracted conveniently. The other is the information of all points in the eight neighborhoods of the point extracted can be used efficiently to reduce the extraction error. The 3×3 mask constructed by rearranging the

coefficients of the CRONE mask according to the 'S' curve is called the 'S' mask, as shown in Figure 9, where a_k (k=1, 2, 3, 4) is the coefficients of the mask. According to the construction of the 'S' curve, this new mask can be converted to the horizontal CRONE mask inversely.

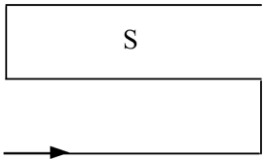

Figure 8. 'S' Curve

$-a_2$	$-a_3$	$-a_4$
$-a_1$	0	$+a_1$
$+a_4$	$+a_3$	$+a_2$

Figure 9. New Mask based on the 'S' Curve

The feature results of Figures 3 (a) and 7 (a) extracted by the 'S' mask are shown in Figures 10 (a) and 11 (a), where m=4 and α=0.55. Under the same conditions, the features extracted by the multi-direction CRONE extraction are shown in Figures 10 (b) and 11 (b), respectively. It can be seen in Figures 10 and 11 that there are more fine features extracted by the 'S' mask than extracted by the multi-direction CRONE extraction. The bus number is clearly seen as 242 in Figure 11(a). However, the extraction of the 'S' mask has a poor performance in the direction of 135 degrees, as shown in Figure 10(a).

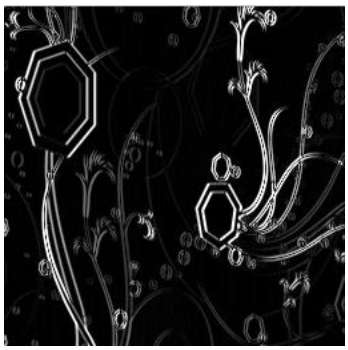

(a) Features extracted by the 'S' mask

(b) Features extracted by the multi-direction CRONE extraction

Figure 10. Feature Extraction Results of Figure 3(a)

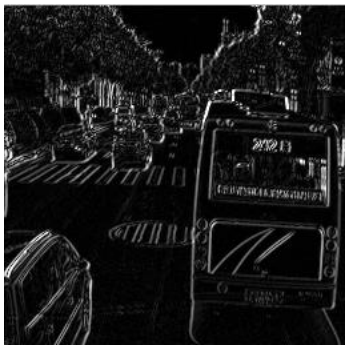

(a) Features extracted by the 'S' mask

(b) Features extracted by the multi-direction CRONE extraction

Figure 11. Feature Extraction Results of Figure 7(a)

3.2. The Improvement of the 'S' Mask

With the combination of the horizontal mask and the vertical mask, the complementary masks, the CRONE mask extracts image features efficiently. Similarly, we will look for a mask complementary to the 'S' mask. As another part of the Peano curve, 'Z' curve is symmetric to the 'S' curve. The direction gaps of both curves are complementary. So as the complementary mask of the 'S' mask, the mask based on the 'Z' curve is constructed, as shown in Fig. 12, to solve the problem that the feature extraction ability of the 'S' mask is weak in a particular direction.

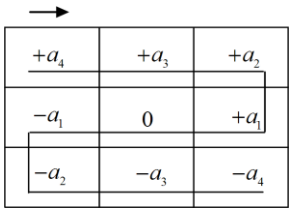

Figure 12. 'Z' Mask based on the 'Z' Curve

The features extracted by the 'S' mask and the 'Z' mask are denoted as G_s and G_z, respectively. The features G_s and G_z are fused and the features extracted by the 'S+Z' mask are then obtained as

$$I = |G_s| + |G_z| . \tag{12}$$

The features of Figures 3 (a) and 7 (a) extracted by the 'S+Z' mask are shown in Figure 13, where m=4 and α=0.55. It can be seen that the features extracted by the 'S+Z' mask are more comprehensive than by the 'S' mask.

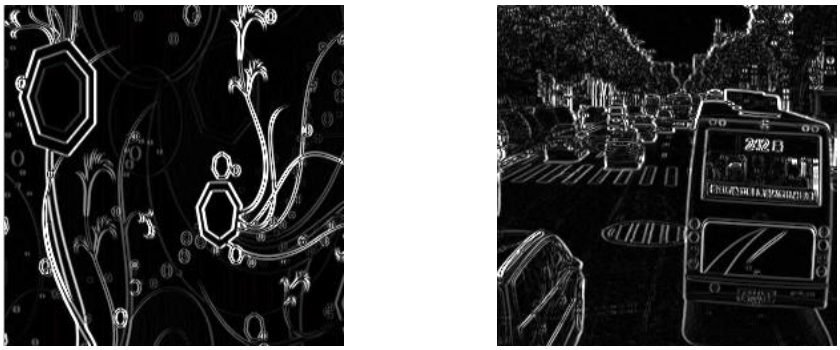

Figure 13. Features of Figures 3 (a) and 7 (a) extracted by the 'S+Z' mask

4. Experimental Analysis

The multi-direction CRONE extraction and the 'S+Z' extraction are applied to extract features of images such as head portrait, ladder, lane and brick, respectively, as shown in Figure 14.

In Figure 14, (a1), (b1), (c1) and (d1) are the feature results of the multi-direction CRONE extraction with α=0.55 and mask length is 5; (a2), (b2), (c2) and (d2) are the feature results of the 'S+Z' extraction with α=0.55 and mask length is 9. From the feature results of the head portrait of Hepburn (Figure 14(a)) and the ladder (Figure 14(b)), we can see that the first method can extract the major features of the image, and the second method extracts the major

features and tiny features at the same time. For example, the features of the ladder extracted by the second method (Figure 14 (b2)) are tiny, lead to that the texture of the ladder is too obvious and the layering of the ladder is thereby too fuzzy. For the lane (Figure 14 (c)), the features extracted by the first method are able to satisfy the needs of traffic scene analysis and the detail features extracted by the second method will generate unnecessary data. For the brick (Figure 14 (d)), the detail features extracted by the second method are convenient for observing the important decorative pattern of the ancient brick, and the features extracted by the first method are too fuzzy to satisfy the demands of the observer.

From the comparisons of the two methods, we can draw the conclusion that the multi-direction CRONE extraction can obtain the outlines of the objects in the images and is suitable in the feature extraction of head portraits and traffic scenes. Also the 'S+Z' extraction extracts features exquisitely and is suitable in the texture feature extraction of images.

(a) Hepburn

(a1) Features extracted by the first method

(a2) Features extracted by the second method

(b) Ladder

(b1) Features extracted by the first method (b2)

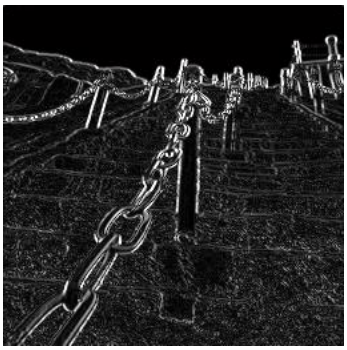

Features extracted by the second method

(c) Lane

(c1) Features extracted by the first method

(c2) Features extracted by the second method

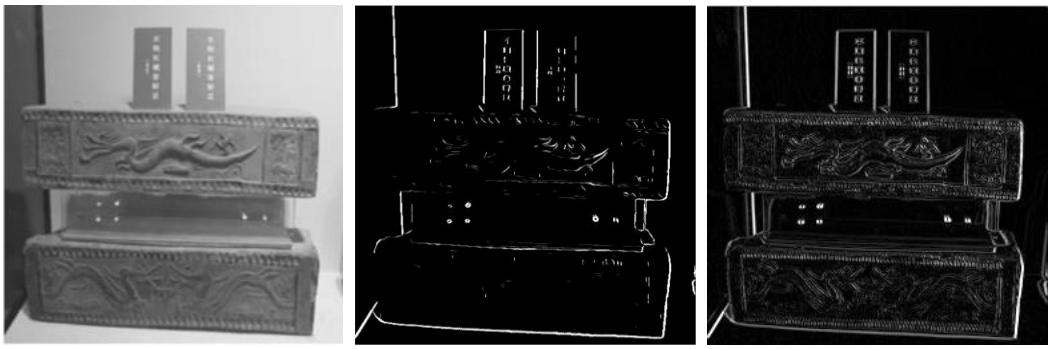

(d) Brick (d1) Features extracted by the first method (d2) Features extracted by the second method

Figure 14. Feature Extraction of Four Images

5. Conclusions

In this paper, based on the fractional differential CRONE operator, two methods for image feature extraction are presented. Experiment results show that the first method, the feature extraction of fusing multi-direction CRONE operators, can extract the outlines of the objects in the image effectively, but has a poor performance in the extraction of the detail information of the image. In order to overcome this shortcoming, the second method, the 'S+Z' extraction combined with the space-filling curves, is presented. Experiment results show that the second method has a good performance in the extraction of the detail information of the image.

The future works will concern on the influence of the fractional order on the image feature extraction, and determine the fractional order adaptively according to the image content to obtain the ideal image feature extraction results.

Acknowledgments

This work is supported in part by the National Natural Science Foundation of China (No. 91120014) and the Foundation of the Education Department of Shaanxi Province (No.12JK0534).

References

[1] K. B. Oldham and J. Spanier, "The fractional calculus", Academic Press, New York, **(1974)**.
[2] B. B. Mandelbrot, "The fractal geometry of nature", W.H. Freeman, New York, **(1982)**.
[3] Y. F. Pu, X. Yuan, K. Liao, Z. L. Chen and J .L. Zhou, "Five numerical algorithms of fractional calculus applied in modern signal analyzing and processing", Journal of Sichuan University, vol. 37, **(2005)**, pp. 118-124.
[4] Z. Z. Yang, J. L. Zhou, M. Huang and X. Y. Yan, "Edge detection based on fractional differential", Journal of Sichuan University , vol. 40, **(2008)**, pp.152-157.
[5] Y. F. Pu, "Fractional calculus approach to texture of digital image", 8th IEEE International Conference on Signal Processing, (**2006)** November 16-20, Beijing, China.
[6] B. Mathieu, P. Melchior, A. Oustaloup and C. Ceyral, "Fractional differentiation for edge detection", Signal Processing, vol. 83, **(2003)**, pp. 2421-2432.
[7] A. Nakib, H. Oulhadj and P. Siarry, "Fractional differentiation and non-Pareto multiobjective optimization for image thresholding", Engineering Applications of Artificial Intelligence, ol. 22, **(2009)**, pp. 236-249.
[8] A. Nakib, Y. Schulze and E. Petit, "Image thresholding framework based on two-dimensional digital fractional integration and Legendre moments", IET image processing, vol. 6, **(2012)**, pp. 717-727.
[9] E. Cuesta, M. Kirane and S. A. Malik, "Image structure preserving denoising using generalized fractional time integrals", Signal Processing, vol. 92, **(2012)**, pp. 553-563.
[10] J. R. Hu, Y. F. Pu and J. L. Zhou, "A novel image denoising algorithm based on riemann-liouville definition", Journal of Computers, vol. 6, **(2011)**, pp. 1332-1338.

[11] J. Che, Y. S. Shi, Y. Xiang and Y. T. Ma, "The fractional differential enhancement of image texture features and its parallel processing optimization", 5th IEEE International Congress on Image and Signal Processing (CISP), (**2012)**, October 16-18, Chongqing, China.
[12] Y. F. Pu, J. L. Zhou and X. Yuan, "Fractional differential mask: a fractional differential-based approach for multiscale texture enhancement", IEEE Transactions on Image Processing, **(2010)**.
[13] G. Huang, L. Xu and Y. F. Pu, "Summary of research on image processing using fractional calculus", Application Research of Computers, vol. 29, **(2012)**, pp. 414-421.
[14] R. Stoica, X. Descombes and J. Zerubia, "Road extraction in remote sensed images using stochastic geometry framework, AIP Conference Proceedings, vol. 568, **(2001)**, pp.531-542.
[15] R. Stoica, X. Descombes and J. Zerubia, "A Gibbs point process for road extraction from remotely sensed images", International Journal of Computer Vision, vol. 57, **(2004)**, pp.121-136.
[16] H. O. Peitgen, H. Jürgens and D. Saupe, "Chaos and fractals: new frontiers of science", Springer, (**2004)**.

